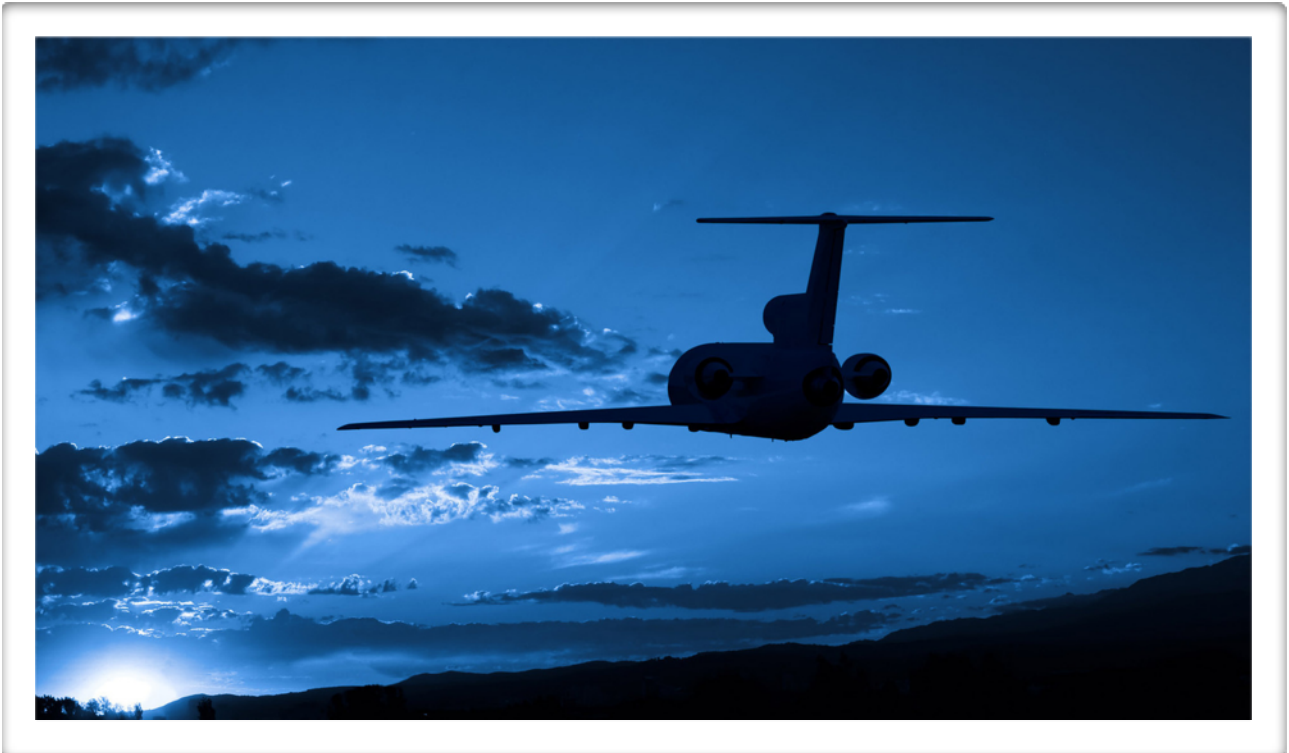# EXTENDED ESSAY

METHODS FOR ANALYTICAL EVALUATION OF AIRPLANES' EFFICIENCY BASED ON THE LIFT-TO-DRAG RATIO

INTERNATIONAL BACCALAUREATE

Subject: *Physics*

Candidate Name: *Ilya Gulko*

Candidate Code: *001414 - 0020*

School: *Bedford School*

Word count: *3985*

Session: *May 2014*

Abstract

In this essay I answer whether it is possible to develop analytical methods on the basis of the lift-to-drag ratio concept through which different airplanes could be compared in terms of their efficiency, actual performance of an individual airplane evaluated against its potential performance and changes in positioning of center of gravity needed to maximise efficiency deduced.

I work with three different models of paper airplanes with characteristic features of the wing: medium aspect ratio & medium profile thickness, low aspect ratio & low thickness and high aspect ratio & high thickness. I propose that by determining the L/D ratio for each of the models over a range of airspeeds and angles of attack and analysing the obtained data I shall be able to determine the most efficient design out of the three, as well as use the results to alter the positioning of center of gravity in each design that would allow the models to perform at their highest potential efficiency.

The research begins with gathering values for lift and drag each model produces at different airspeeds and angles of attack. The data is processed to obtain values for the lift-to-drag ratio and the total aerodynamic force at every combination of airspeed and angle of attack. The two sets of data are then used together to build a curve for each paper airplane that reflects its performance in air when the angle of attack is not fixed. The peaks of these curves indicate the maximum potential efficiency achieved by a design with known mass, which is verified in a supplementary experiment.

I conclude that methods to use the L/D ratio concept for analytical evaluation of efficiency indeed exist and indicate questions arisen by the work done which fell beyond the scope of this essay.

Word count: 298

Table of Contents

1. Introduction

Efficiency is amidst the central concerns for a vast majority of current developments in the aviation industry of today. An efficient design allows an airplane to generate the necessary lift with lower energy consumption, and in the context of energy crisis anticipation, reduction of energy requirements for air transport is crucial. Success has been made in the industry over the last half a century: over-70% overall improvement since 1960 is claimed[1]. Besides a leap in engine fuel per unit thrust, reduction in aerodynamic drag was a major contributor in that change[2]. In most recent years the focus of research in efficiency enhancement has shifted towards reduction of airplanes' mass through use of lightweight materials.

The entire amount (or one nearing it) of useful energy put into thrust is used to overcome the aerodynamic drag acting on the airplane[3]. Generally lift tends to be proportional to drag in a particular flight regime[4], and so one realizes that the more lift can be created per unit of drag experienced - the greater efficiency an airplane can achieve. This concept is summarized by the lift-to-drag ratio, usually referred to as the *L/D ratio*, which can serve as an indicator of an airplane's efficiency[5]. I will attempt to answer whether it is possible to develop analytical methods on the basis of the lift-to-drag ratio concept through which different airplanes could be compared in terms of their efficiency, actual performance of an individual airplane evaluated against its potential performance and changes in positioning of center of gravity to improve efficiency deduced.

Efficiency of an airplane design could be maximised by ensuring its efficient performance as a glider. Airplane origami, also called *aerogami*, is vastly popular for ease of build and the wide variety of designs, which makes paper airplanes attractive to me as the subjects of my research. In addition, in the context of this work paper gliders hold advantage over scaled models of larger aircraft, in that applying data obtained for them to real world situations would not require conversions to compensate for difference in Reynolds numbers due to size, which will be explained later in this work.

---

[1] Peeters and Middel et al., 2005, p. 7

[2] Peeters and Middel et al., 2005, p. 10

[3] Moran, 1984

[4] Capehart, 2007

[5] Grc.nasa.gov, 2013

2. Definitions of terms

Aerodynamic force - a force acting on a body as a result of its motion through gas.

Aerodynamic lift, also *lift* - the component of the aerodynamic forces acting on the wing or airfoil section that opposes gravity[6].

Aerodynamic drag, also *drag* - the component of aerodynamic forces acting on the wing or the airfoil section, which is parallel and opposite to the relative airflow[7].

Cruise condition of flight - a particular flight condition, whereas the aircraft is moving at constant velocity, i.e. all the forces acting on it balance.

Angle of attack, also *angle of incidence* - the angle between the chord of the wing's airfoil and the direction of flight.

Chord - the distance between the leading edge and the trailing edge of an airfoil measured parallel to the fuselage central line.

---

[6] 'lift' 2004, in An Illustrated Dictionary of Aviation, McGraw-Hill, New York, NY, USA, viewed 03 December 2013

[7] 'drag' 2004, in An Illustrated Dictionary of Aviation, McGraw-Hill, New York, NY, USA, viewed 03 December 2013

3. Prior knowledge and proposal

3.1 Balance of forces in cruise conditions for motored aircraft

The major forces acting on any airplane in flight are thrust, drag, weight and lift, and in order for the aircraft to fly at constant velocity, all of these forces have to be balanced, according to Newton's first law of motion. In case of the plane traveling with constant velocity parallel to horizon, the forces align in balanced pairs as shown on fig.1: thrust and drag act along the horizontal, whilst lift and weight act along the vertical. On fig.1 L, W, T and D stand for the forces of lift, drag, thrust and weight respectively. Provided that there are no external influences, the total aerodynamic force R is the vector sum of L and D and is balanced by the vector sum of T and W.

Fig.1 - Balance of forces in flight
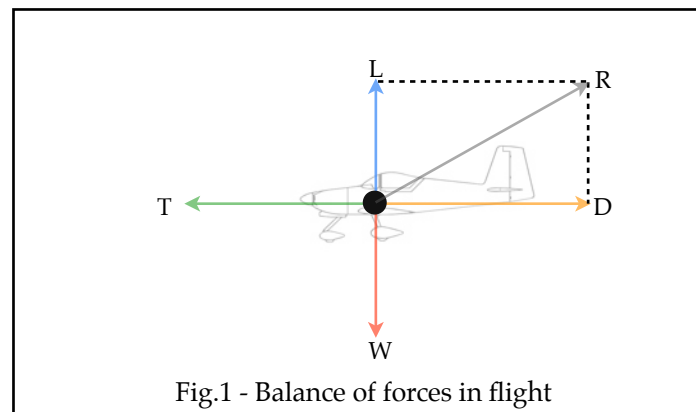
3.2 Balance of forces in cruise conditions for gliders

In the case of the powered airplanes R is overcome through the use of the weight of the aircraft and the power of its engines. Having no engines, gliders have to rely solely on their weight to balance R, meaning that in order to achieve a constant velocity in flight, the glider must have its R directed vertically upwards, opposite to the action of weight. With this in mind, we illustrate the balance of forces in a gliding flight, and fig.2 shows how the weight W of the glider balances the aerodynamic force R acting on it. Notice that thrust T is being provided as a component of W.

Fig.2 - Balance of forces in gliding flight
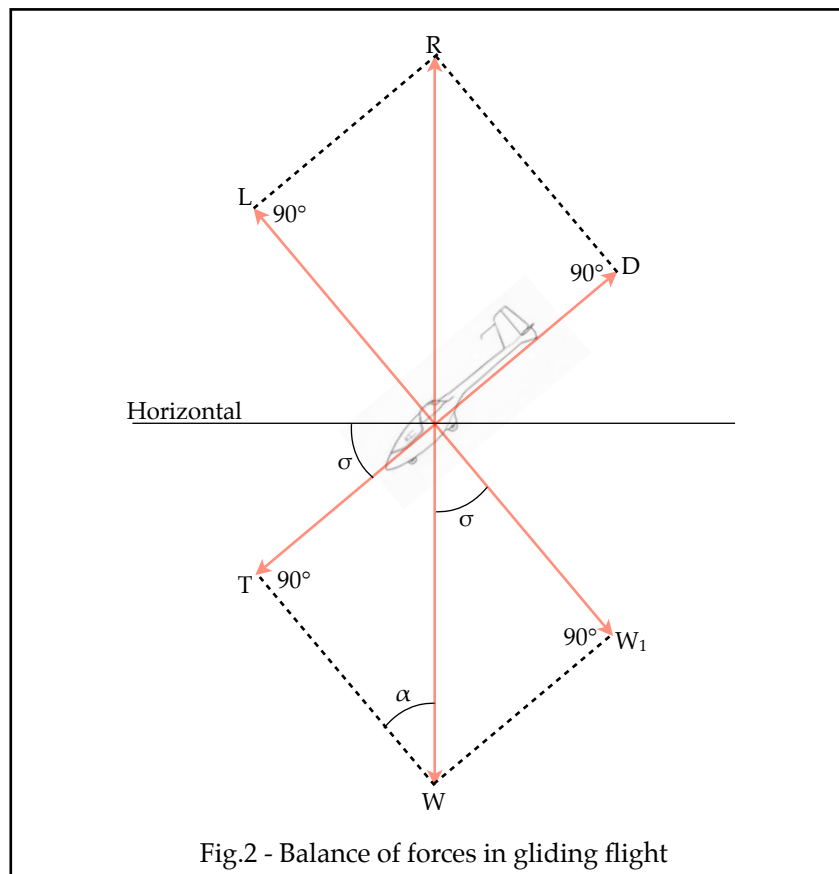
3.3 Significance of L/D for gliders

With reference to fig.2, we use trigonometry of a right triangle to deduce that when a glider is in its normal mode of flight and flying at an angle σ to the horizon, $W_1 = W\cos\sigma$ and $T = W\sin\sigma$. Because T and W_1 are balanced by D and L respectively (Newton's first law of motion), this can be rewritten as $L = W\cos\sigma$ and $D = W\sin\sigma$. Substituting this into the lift-to drag ratio, we obtain:

$$L/D = W\cos\sigma(W\sin\sigma)^{-1}$$

$$\therefore L/D = \tan^{-1}\sigma$$

But $\tan^{-1}\sigma$ is the ratio of total horizontal distance crossed to initial height, and so:

$$L/D = \Delta S \Delta h^{-1}$$

where ΔS = change in horizontal distance and Δh = change in height

This observation is useful, as it allows to use the L/D ratio to calculate the efficiency of a glider as follows:

$$\Delta S \Delta E^{-1} = (L/D\Delta h)mg\Delta h^{-1}$$

$$\therefore \Delta S \Delta E^{-1} = L/D(mg)^{-1}$$

where ΔS = change in horizontal distance, ΔE = loss in potential energy, m = mass of the glider and g = acceleration of free fall

3.4 Limits to paper glider's L/D ratio due to low Reynolds number

Small airplanes, especially the paper gliders, experience a proportionally much higher drag than the full-scale airplanes. This is explained by increased significance of viscous forces generated by air.

Viscosity is the tendency of a fluid to resist sliding between layers[8]. Kinematic viscosity *v* is commonly used in calculations as the indicator of viscosity[9].

The significance of the fluid's viscosity in a particular situation can be quantified using the Reynolds number *Re*, a dimensionless number that establishes the proportionality between the fluid inertia and the sheer stress as a result of viscosity[10]. The higher the Reynolds number is - the less significant effect the fluid's viscosity has.

If v is the relative velocity of flow and L is a characteristic length over which *Re* is measured, e.g. the chord of a wing, the Reynolds number is calculated using:

$$\text{Re} = \frac{\text{inertial forces}}{\text{viscous forces}} = \frac{\rho \mathbf{v} L}{\mu} = \frac{\mathbf{v} L}{\nu}$$

(Image retrieved from: Wikipedia. 2013. Reynolds number. [online] Available at:
http://en.wikipedia.org/wiki/Reynolds_number [Accessed: 30 Nov 2013].)

Due to its proportionality to characteristic length, the *Re* of A4 paper gliders will be substantially lower than that of full-scale airplanes. Thus, assuming room temperature[11], airspeed of 4 ms^{-1} and characteristic length (chord) of 0.2 m, for the wing of a paper airplane the value is roughly 51,020, whilst the wings of a four passenger airplane can have an *Re* of up to about 6,000,000[12]. A

---

[8] Houghton and Carpenter, 2003, p. 8

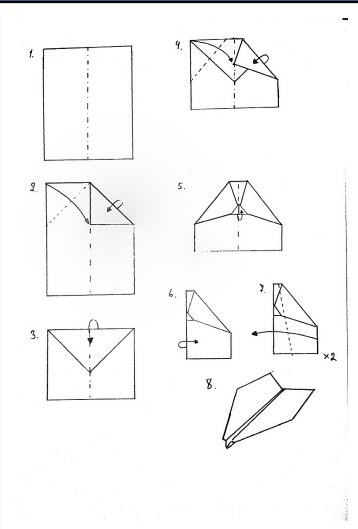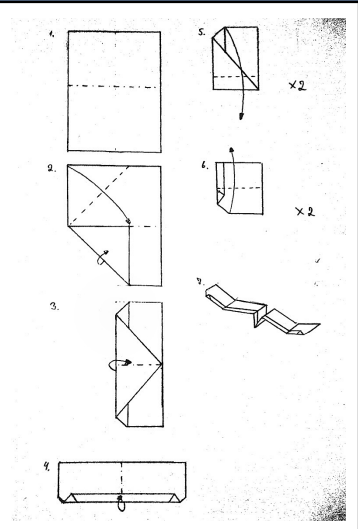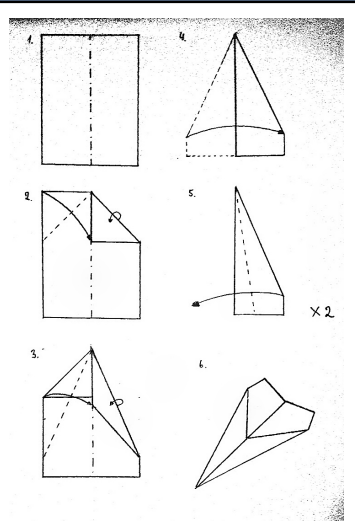[9] Houghton and Carpenter, 2003, p. 9

[10] 'Reynolds number' 2004, in An Illustrated Dictionary of Aviation, McGraw-Hill, New York, NY, USA, viewed 7th September 2013

[11] At 27°C kinematic viscosity of air is 15,68×10^{-6} m^2/s (Engineeringtoolbox.com, 2013)

[12] Backburn, 2013

small Reynolds number means that viscosity of air has a much greater effect over the paper airplane, resulting in increased drag and worsened lift[13], resulting in low L/D ratio In fact, based on the results of the experiment I carried out for this work, I do not believe that an L/D ratio higher than about 12:1 is achievable with origami paper gliders.

3.5 The choice of paper airplane models

	'CLASSIC'	'SLOW'	'DART'
INSTRUC-TIONS			
	original illustrations		
FEATURES OF THE WING	Low aspect ratio and swept-back with airfoil of medium thickness	High aspect ratio with no sweep angle but thick-profile airfoil	Very low aspect ratio with a large sweep-back angle and thin-profile airfoil

3.6 Proposal

I expect that by determining the L/D ratio for each of the models over a range of airspeeds and angles of attack and analysing the obtained data I will be able to determine the most efficient design out of the three, as well as use the results to adjust the positioning of center of gravity of the models that would increase their efficiency.

---

[13] Backburn, 2013

4. Testing the proposal

4.1 Setting quantitative boundaries for the testing

A brief preliminary experiment was conducted to determine the quantitative boundaries for airspeeds. In the experiment plain office A4 paper was used to build airplanes of the chosen designs, and the models were launched from hand from an approximately known height with minimum initial speed, and their time aloft was taken using a stopwatch. The horizontal distance they crossed was measured from the point on the ground beneath the point of release. Using the data obtained, the total distance each model crossed was found using Pythagoreans theorem and division of the result by the airtime produced the value for speed. The data collected in this experiment is given in the *Table a* of the appendix.

Even though errors to the method are not considered here, it must be appreciated that there is a large uncertainty to readings of both the average airspeeds and the L/D ratios. Though, the role of this experiment is only to give impression of the possible speeds, which was successfully achieved, and so we do not concern ourselves with quantifying the errors. The airspeeds of $1ms^{-1}$, $2ms^{-1}$, $3ms^{-1}$, $4ms^{-1}$ and $5ms^{-1}$ were chosen for the main experiment.

The range for angle of attack could be deduced experimentally, by filming each flight and then using software to analyse each frame. However, this method was seen too time-consuming, and the range was selected intuitively. It was decided to start testing with -4° and gradually increase the angle with increment of 4° until 16°.

4.2 Designing methods to measure lift and drag at varying airspeed and angle of attack

A wind tunnel was used to simulate flow of air around the paper airplanes in flight. The one I used allowed to set the speed of rotation of the fan to a particular frequency. Preliminarily I determined the frequencies that corresponded to the airspeeds I was to test at by placing an anemometer on its own into the wind tunnel and recording the needed data. The results were later used during testing and are shown in *Table c* of the appendix.

In order to be able to set the angle of attack to particular values, I have designed a mount that is shown in fig.3 below: the airplane is fixed in a specially suited clam, which is attached to a mount that is made up of two segments joint by a bolt as shown in fig.4, the upper segment being placed over the lower one. An analogue protractor is fixed to the lower segment, and a needle

sticking out of the bottom of the upper one indicates a specific angle on it, that angle being the an-gle of attack, provided that the perpendicular to the needle is parallel to the airplane's wing's chord. This assembly has been used to set the angle of attack both in the measurement of lift and in that of drag.
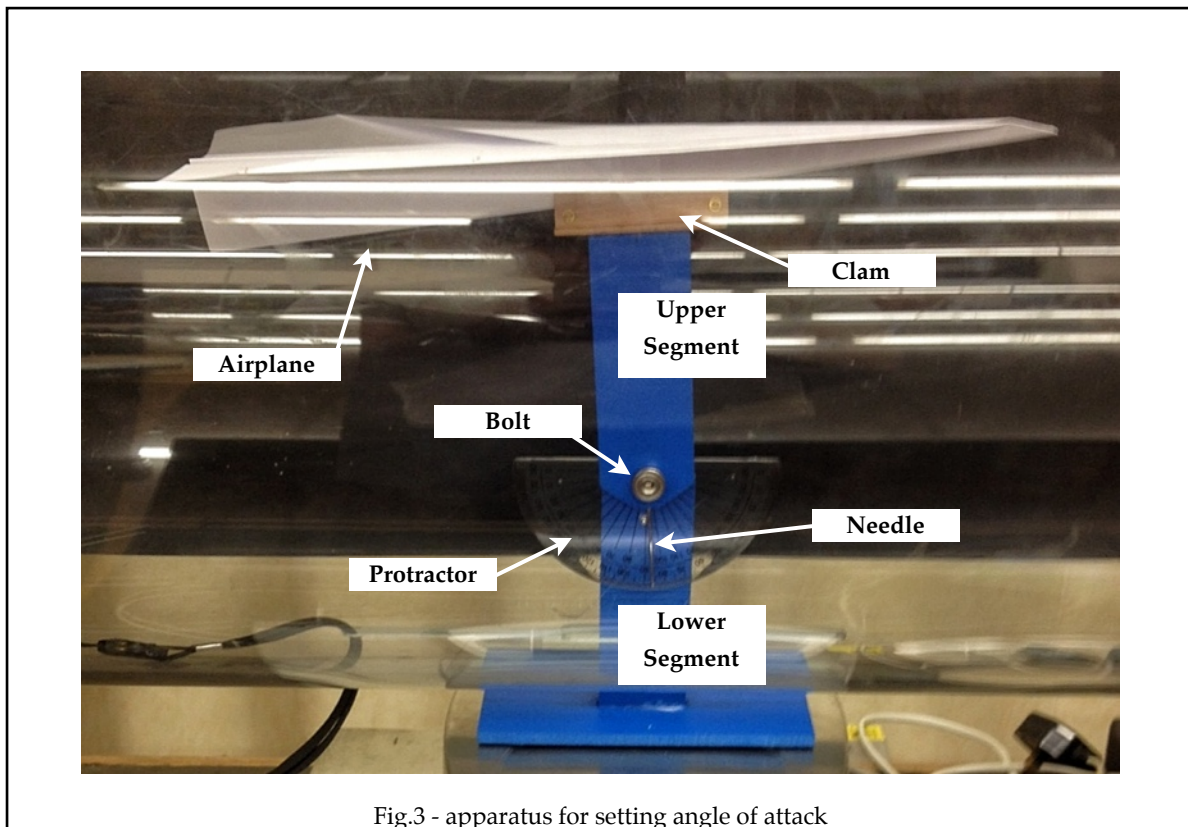

Fig.3 - apparatus for setting angle of attack

The testing of each model took place in runs. During each run the angle of attack was kept constant and the airspeed was varied either from the smallest to the largest or in the other way.

Lift was measured by attaching the assembly to a balance, so that the airplane became lo-cated in the wind tunnel. The balance was zeroed with the assembly holding the airplane on it be-fore each run, prior to turning the power on, and then during the runs the values opposite to those given by the balance were taken for lift.

The apparatus used to measure drag is shown on the diagram in fig.4: the assembly for set-ting the angle of attack was mounted on a cart that was allowed to slide along a track. A thread and a pulley were used to redirect the pressure of drag to a balance: the string was attached to the cart on one end, guided over a pulley and fixed to a balance on the other end. In addition, the track was inclined in direction of the action of drag, to minimise the effects of friction. The angle of incli-nation was 5°, which was later subtracted form the readings of angle of attack.
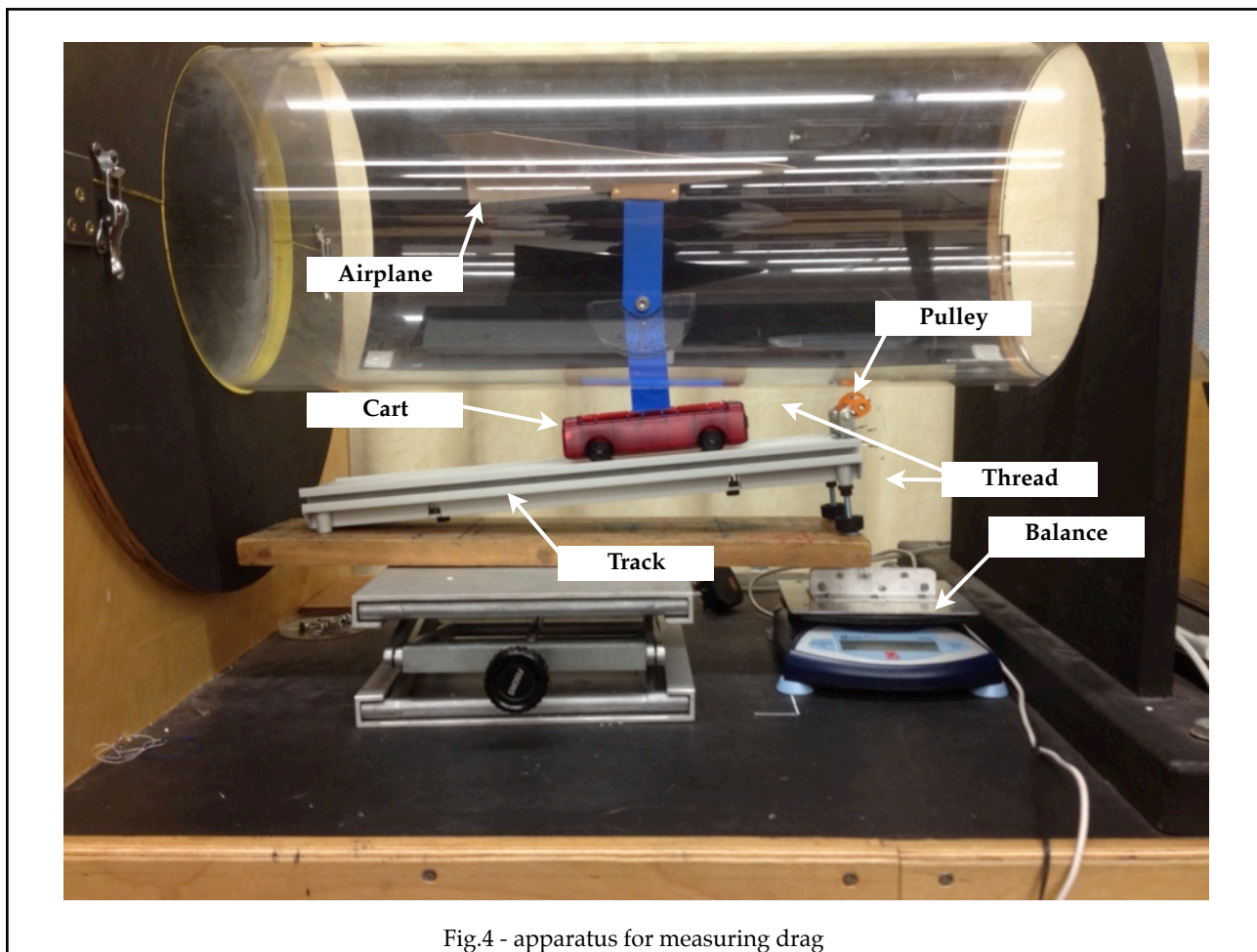
Fig.4 - apparatus for measuring drag

4.3 Appreciating potential errors and minimizing them

Sources of potential errors include the following:

• inaccurate measurement of angle of attack

• inaccurate measurement of lift

• inaccurate measurement of drag

• inaccurate measurement of airspeed

• turbulent flows of external origin

• gradual wear of the paper model under test

In order to reduce the error to the measurement of angle of attack, a set square was used to align the chord of each airplane's wing with the perpendicular to the needle on the upper segment of the mount. However, a naked eye was used to check for alignment, lending to potential random

errors, and also the lower surface of the wing was approximated to be parallel to the chord, which has potential to systematically increase the angle of attack for every step of the experiment, especially for the 'SLOW' model with a thick-profile airfoil.

The errors in the measurement of the angle of attack cause errors to the measurements of lift and drag. These errors cannot be eliminated, however the random error was reduced by keeping the hold of the airplane in the clam unaltered until all necessary data for the specific model was collected. Nevertheless, a random error of parallax could occur when changing the angle of attack during each models' testing.

Other than for the reason described above, the inaccuracy to drag could be introduced by the friction forces between the cart and the track. In addition, high presence of random errors has been observed during the first runs, which I blamed on the imperfections in the round shape of the wheels of the cart. The significance of both was minimised through overcompensation, by inclining the track towards the action of drag. In order to avoid the component of weight contributing to the reading of drag, it was crucial to zero the balance precisely at the point of equilibrium at $0ms^{-1}$ airspeed. To achieve this, prior to zeroing the balance the airspeed was turned to a value just higher than $5ms^{-1}$ and then gradually decreased to $0ms^{-1}$. With such procedure, after every run the reading on the balance came back to zero, which shows that the initial position was the equilibrium.

The procedure for controlling the airspeed was only done once, before the experiment, and any changes to the airspeed-frequency relation that could take place onwards were not accounted for. It is, however, not expected that these variations, if any, would be significant.

Turbulent flows of external origin would have distorted the measurements and increased the fluctuation of the reading on the balance, leading to increased difficulty taking the middle value. However, the configuration of the wind tunnel, whereas the fan is located in the back, sucking the air into the tunnel through a flow-straightening filter, minimised the amount of turbulent flows. Nevertheless, there were edges on the tunnel's inner surface in front of the position of the model, as well as holes to let the measuring equipment and supports inside. Both could potentially produce eddies. Additional turbulence was caused by the mount for the paper airplanes itself and I expect this source to be visible in the data for the 'DART' plane.

To fight the issue of wear, for tests in the wind tunnel I used specimen built with card. To the best of my ability I ensured that the aerodynamic characteristics remained uninfluenced by increased thickness of the material.

The work aims to suggest an evaluative approach, rather than to work closely with quantities, and the aim would be fulfilled as far as the predictions based on the suggested mathematical

model seem to work in real life. For this reason uncertainties will not be considered in data processing. Errors due to measuring equipment can be found in *Table b* in the appendix.

4.4 Data collection

Alongside the values for L and D uncertainty caused by the fluctuation of the reading on the balance was noted. Please see tables #1, #3 and #5 of the appendix for raw data. <u>Please note that due to specificities of the software used, commas are used as decimal marks throughout the materials in the appendix.</u>

4.5 Data processing

As mentioned already, it is not necessary under the aim behind the experiment to take quantitive account of errors in the evaluation of data.

Firstly, note that fluctuations to the readings increase with growing airspeed strongly for the 'DART' model, which confirms my expectations of the influence of drag induced by the mount.

The first calculation that needs to be done is to find the real value of drag for every speed and angle of attack, as the reading was distorted by the method used. I resolve forces into vertical and horizontal components and use trigonometry of right triangle to deduce that:

$$D_{real} = (Lsin\beta + D_{raw})\,cos^{-1}\beta$$

Tables #2, #4 and #6 quote D_{real} for D.

Quantities of L/D *(=LD⁻¹)* and *R* are of interest to us. They are calculated, and their values displayed in the respective columns of the tables.

Charts #1 through *#6* show plots of *R* and *L/D against airspeed* for the angles of attack tested. Data has been omitted whenever negative lift was created, which resulting in a negative L/D ratio. It is noted that the rest of the series in all cases clearly form a curve, so software is used to build one for each series. No anomalous readings have been noticed.

4.6 Evaluation of efficiency through working with R and L/D

It is noted that L/D is not constant, but varies with both the airspeed and the angle of attack. Means are needed to deduce the maximum possible L/D ratio at the range of speeds and angles of attack considered.

To start with, the charts for *R against airspeed* are placed above the ones for *L/D against airspeed* as shown on *chart #7* with data for 'CLASSIC' model copied here from the appendix as an example. One sees that if mass of the paper airplane is known, it is possible to find from the graphs for *R* the airspeed the airplane will require to compensate for its weight with *R,* at each fixed angle of attack. Models tested in the preliminary experiment were folded of identical paper sheets and all weighed 5g. A line parallel to the axis for airspeed is drawn, and the equilibrium airspeed for each angle of attack is then given by the x-coordinate of the corresponding points of intersections. The vertical dotted lines are extended towards the bottom axis, so that they intersect with their respective plots of L/D against airspeed *(e.g. the vertical drawn from the intersection point on the R plot for 16° must intersect the plot of L/D for 16°, and for this particular vertical that is the only intersection that is noted)*. The y-coordinates of the latter intersections now tell us the value of L/D at certain airspeeds and angles of attack for a particular model. Plotting a curve through the points of intersection, we build a new plot that shows the variation of L/D against airspeed for a particular model at an uncontrolled angle of attack, i.e. in case the model is allowed to stabilize itself freely in air. The idea behind the curve is based on the assumption that at every instance of flight the net force acting on the model is zero, which in real flight is not always the case. However, because of the low mass of the paper airplanes, such approach would be a very good approximation. At the peaks of the obtained plots the efficiency of each particular glider is theoretically at its greatest.

The same procedure is repeated for data gathered for the remaining models and the produced graphs are placed into side by side comparison in *Chart #10*, also copied to here from the appendix.

Chart #7: Building L/D curve for the case of uncontrolled engle of attack for 'CLASSIC' model; mass = 5g

Chart #10: Comparison of L/D curves for the three models

L/D ratio versus airspeed for 'CLASSIC' model

L/D ratio versus airspeed for 'SLOW' model

L/D ratio versus airspeed for 'DART' model

Legend:
— α = -4° — α = 0° — α = 4° — α = 8° — α = 12° — α = 16° ◆ α = variable
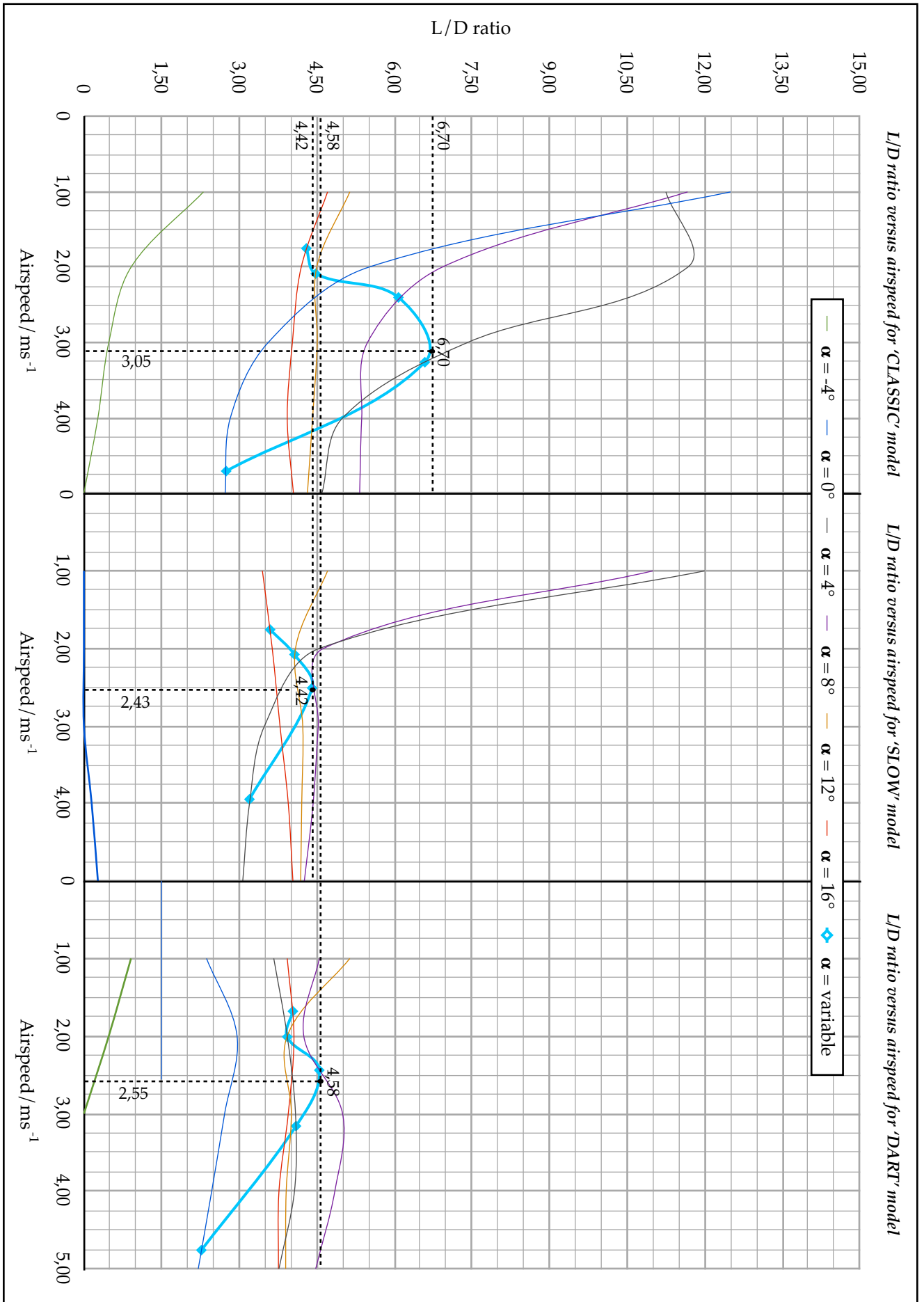
5. Conclusion

5.1 Review of proposals in the light of the work done

The first observation we make from *Chart #10* is that the 'CLASSIC' model seems to be capable of achieving a much higher efficiency than the other two models. However, in the preliminary experiment this model was observed to have speed fluctuating around roughly 4.30 ms^{-1} and lift-to-drag ratio of approximately 3.00, which is below the experimentally estimated L/D ratio for the 'SLOW' model and substantially lower than 6.70 suggested by the plot. This either means that the model is not operating at its greatest efficiency or that the method produces false results. Counter evidence to the second is already given by the peak of the graph for the 'SLOW' model approximately corresponding to the experimental values for that airplane. This evidence, though, does not exclude the possibility of the second.

It was observed in practice and on the graph that the model flies at an angle of attack close to 0°. The angles of attack are seen to decrease along the plots from left to right, and for the 'CLASSIC' model peak on the plot occurs at an angle of attack just greater than 4°. Increase in the angle of attack could be achieved by shifting the center of gravity further aft. If this alteration can improve the efficiency of the model in the experiment, the validity of the evaluation method would be confirmed.

By attaching a paper clip to the back of the 'CLASSIC' plane and thus shifting the center of gravity backwards, I was able to markedly extend the range of flight. This result confirms the validity of the method suggested.

Following the same procedure for the 'DART' model and making the same change also resulted in improvement of its efficiency, however adjustment of center of gravity position did not improve the performance of the 'SLOW' model, which is consistent with its original version already flying at its maximum potential efficiency as shown by its L/D curve. The expectations outlined in the proposal were confirmed.

5.2 Link to research question

Returning back to the research question, I devised methods that rely on the L/D ratio concept that allow for comparison between several airplanes in respect to their maximum potential efficiency, provide means to evaluate whether the airplane is performing at its highest potential

efficiency and that I could use to reposition the center of gravity of some models in a way that noticeably improved their efficiency. I therefore give an affirmative answer to the research question.

5.3 Limitations and further research

In this work I was constrained mainly by the word limit. If it was not in place, I would have researched further to build another set of curves to reflect the correlation between the L/D ratio and the angle of attack and evaluate its usefulness in analysis of an airplane's design. I would also have attempted to establish a relationship between the position of the center of gravity and the angle of attack in cruise conditions during flight. I would suggest these topics for further study and research.

6. Bibliography

Websites:

Backburn, K. 2013. Paper Airplanes. [online] Available at:
http://www.paperplane.org/paero.htm [Accessed: 30 Nov 2013].

Engineeringtoolbox.com. 2013. Air - Absolute and Kinematic Viscosity. [online] Available
at: http://www.engineeringtoolbox.com/air-absolute-kinematic-viscosity-d_601.html [Accessed: 30 Nov 2013].

SmartPlanet. 2013. A sharkskin coating for ships, planes and blades. [online] Available at:
http://www.smartplanet.com/blog/intelligent-energy/a-sharkskin-coating-for-ships-planes-and-blades/ [Accessed: 2 Dec 2013].

Grc.nasa.gov. 2013. L/D Ratio. [online] Available at:
http://www.grc.nasa.gov/WWW/k-12/airplane/ldrat.html [Accessed: 30 Nov 2013].

Books:

Capehart, B. 2007. Encyclopedia of energy engineering and technology. Boca Raton, FL:
CRC Press.

Houghton, E. and Carpenter, P. 2003.Aerodynamics for engineering students. Oxford:
Butterworth-Heinemann.

Moran, J. 1984. An introduction to theoretical and computational aerodynamics. New York:
Wiley.

Peeters, P., Middel, J. and Hoolhorst, A. 2005. Fuel efficiency of commercial aircraft. An
overview of historical and future trends.

Potter, M., Wiggert, D. and Hondzo, M. 2002.Mechanics of fluids. Pacific Grove, CA: Brooks
Cole /Thompson Learning.

EXTENDED ESSAY

APPENDIX

METHODS FOR ANALYTICAL EVALUATION OF AIRPLANES' EFFICIENCY BASED ON THE LIFT-TO-DRAG RATIO

Bedford School

Ilya Gulko (0001414 - 0020)

Contents:

Tables:

Charts:

Table b: Uncertainties due to measuring equipment errors

EQUIPMENT	QUANTITY MEASURED AND UNITS	UNCERTAINTY
Analogue ruler*	Length/m	±0,0005
Analogue protractor*	Angle/deg	±0,5
Digital balance**	Force/g	±0,1
Digital anemometer**	Airspeed/ms⁻¹	±0,01
Digital frequency indicator**	Frequency of the fan's rotation/Hz	±0,1

*± half of smallest division for analogue instruments
**± one smallest division for digital

Table c: Frequency settings corresponding to particular airspeeds

AIRSPEED	FREQUENCY
1 ms⁻¹	7,0 Hz
2 ms⁻¹	10,5 Hz
3 ms⁻¹	14,5 Hz
4 ms⁻¹	18,1 Hz
5 ms⁻¹	22,8 Hz

Table a: Raw data and estimated average airspeed of the three models

MODEL	HORIZONTAL DISTANCE/m	HEIGHT /m	TIME /s	TOTAL DISTANCE /m	AVERAGE SPEED/ms⁻¹	APPROXIMATE L/D RATIO
'CLASSIC'	4,70	1,59	1,13	4,96	4,39	2,96
	5,93	1,59	1,62	6,14	3,79	3,73
	3,75	1,59	0,92	4,07	4,43	2,36
	4,60	1,59	1,11	4,87	4,38	2,89
	4,43	1,59	1,13	4,71	4,17	2,79
'SLOW'	5,65	1,51	2,60	5,85	2,25	3,74
	6,75	1,51	2,77	6,92	2,50	4,47
	6,88	1,51	2,97	7,04	2,37	4,56
	6,92	1,51	3,01	7,08	2,35	4,58
	5,97	1,51	2,71	6,16	2,27	3,95
'DART'	1,68	4,18	0,81	4,50	5,56	0,40
	1,79	4,18	0,91	4,55	5,00	0,43
	1,87	4,18	0,86	4,58	5,32	0,45
	1,87	4,18	0,81	4,58	5,65	0,45
	1,80	4,18	0,79	4,55	5,76	0,43

'CLASSIC' model:

Table #1: Raw Data for 'CLASSIC' model

α → AIRSPEED ↓	-4°				0°				4°				8°				12°				16°			
	L/g	±L	D/g	±D	L/g	±L	D/g	±D	L/g	±L	D/g	±D	L/g	±L	D/g	±D	L/g	±L	D/g	±D	L/g	±L	D/g	±D
1 ms⁻¹	0,30	0,00	0,10	0,00	0,50	0,00	0,00	0,00	0,90	0,00	0,00	0,00	1,40	0,10	0,00	0,00	1,90	0,10	0,20	0,00	2,40	0,10	0,30	0,00
2 ms⁻¹	0,30	0,00	0,30	0,00	1,10	0,00	0,10	0,00	2,10	0,10	0,00	0,00	3,60	0,20	0,20	0,00	4,50	0,10	0,60	0,00	6,00	0,20	0,90	0,00
3 ms⁻¹	0,30	0,10	0,60	0,00	2,10	0,10	0,40	0,00	4,30	0,10	0,20	0,00	7,40	0,10	0,70	0,00	9,70	0,20	1,30	0,00	12,50	0,30	2,00	0,10
4 ms⁻¹	0,30	0,10	1,10	0,00	3,40	0,10	0,90	0,00	7,10	0,20	0,80	1,00	12,20	0,20	1,20	0,10	15,90	0,30	2,20	0,00	20,50	0,40	3,40	0,00
5 ms⁻¹	0,00	0,00	1,90	0,00	5,40	0,10	1,50	0,00	11,60	0,20	1,50	0,10	20,10	0,30	2,00	0,10	25,80	0,40	3,70	0,10	33,30	0,40	5,30	0,20

Table #2: Processed data for 'CLASSIC' model

α → AIRSPEED ↓	-4°				0°				4°				8°				12°				16°			
	L/g	D/g	LD⁻¹	R/g	L/g	D/g	LD⁻¹	R/g	L/g	D/g	LD⁻¹	R/g	L/g	D/g	LD⁻¹	R/g	L/g	D/g	LD⁻¹	R/g	L/g	D/g	LD⁻¹	R/g
1 ms⁻¹	0,30	0,13	2,31	0,33	0,50	0,04	12,50	0,50	0,90	0,08	11,25	0,90	1,40	0,12	11,67	1,41	1,90	0,37	5,14	1,94	2,40	0,51	4,71	2,45
2 ms⁻¹	0,30	0,33	0,91	0,45	1,10	0,20	5,50	1,12	2,10	0,18	11,67	2,11	3,60	0,52	6,92	3,64	4,50	1,00	4,50	4,61	6,00	1,43	4,20	6,17
3 ms⁻¹	0,30	0,63	0,48	0,70	2,10	0,59	3,56	2,18	4,30	0,58	7,41	4,34	7,40	1,35	5,48	7,52	9,70	2,15	4,51	9,94	12,50	3,10	4,03	12,88
4 ms⁻¹	0,30	1,13	0,27	1,17	3,40	1,20	2,83	3,61	7,10	1,42	5,00	7,24	12,20	2,27	5,37	12,41	15,90	3,60	4,42	16,30	20,50	5,21	3,93	21,15
5 ms⁻¹	0,00	1,91	0,00	1,91	5,40	1,98	2,73	5,75	11,60	2,52	4,60	11,87	20,10	3,77	5,33	20,45	25,80	5,97	4,32	26,48	33,30	8,23	4,05	34,30

Chart #1: R versus airspeed for 'CLASSIC' model
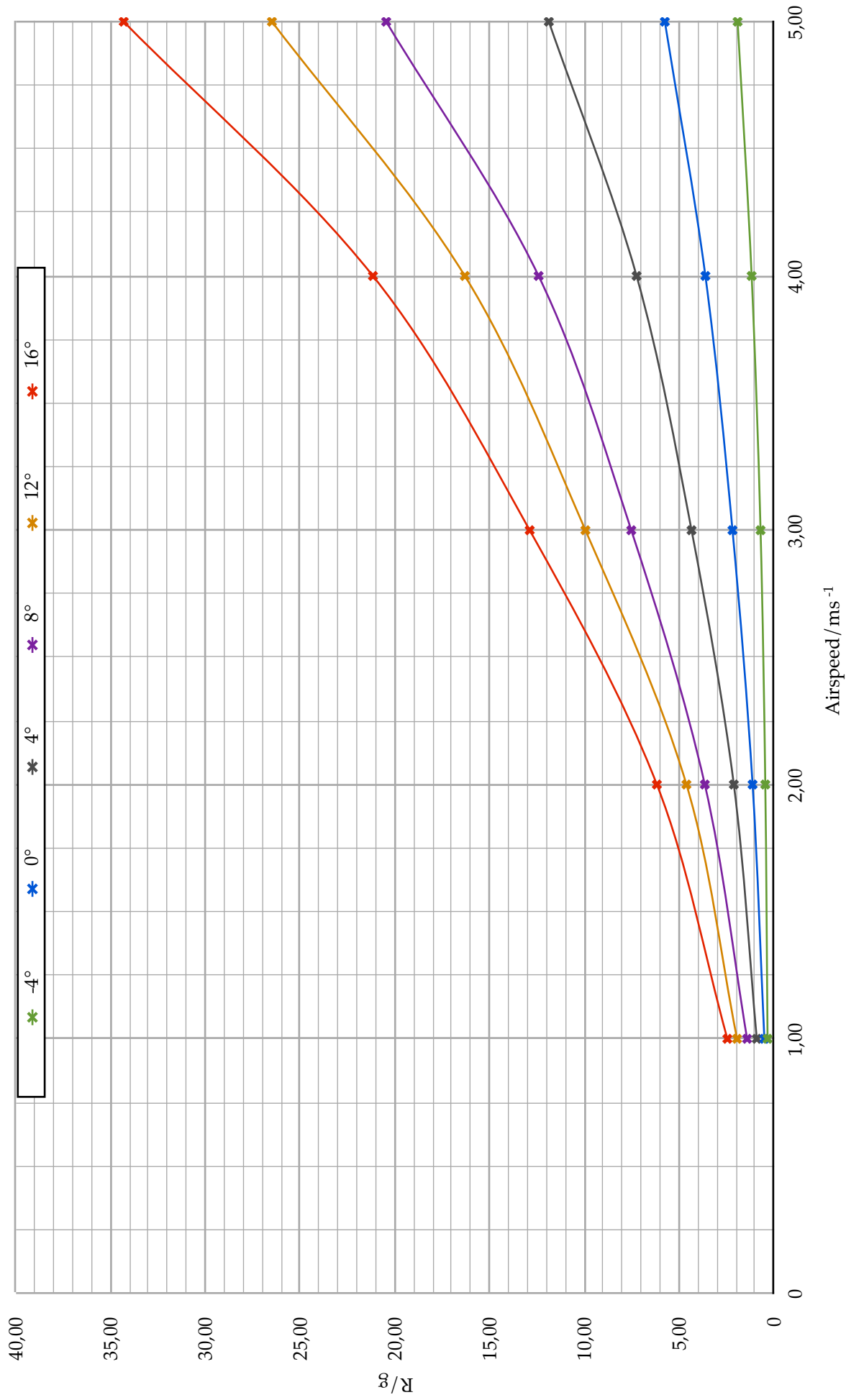
Chart #2: *L/D ratio versus airspeed for 'CLASSIC' model*
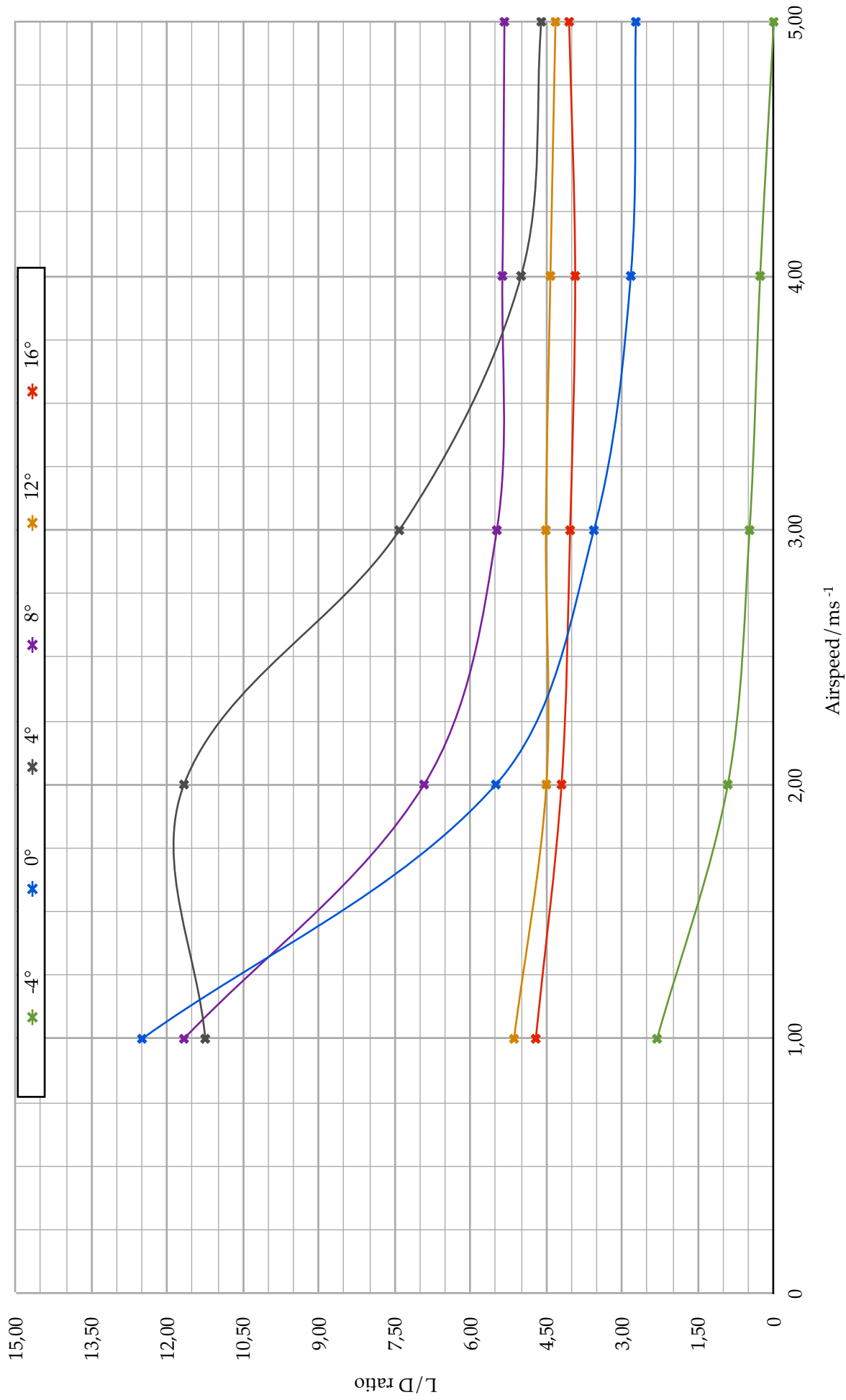
'SLOW' model:

Table #3: Raw data for 'SLOW' model

AIRSPEED	-4°				0°				4°				8°				12°				16°			
α →	L/g	D/g	±L	±D	L/g	D/g	±L	±D	L/g	D/g	±L	±D	L/g	D/g	±L	±D	L/g	D/g	±L	±D	L/g	D/g	±L	±D
1 ms⁻¹	-0,50	0,30	0,00	0,00	0,00	0,20	0,00	0,00	0,60	0,00	0,00	0,00	1,10	0,00	0,10	0,00	1,60	0,20	0,00	0,00	2,00	0,40	0,10	0,00
2 ms⁻¹	-1,90	0,60	0,00	0,00	0,00	0,40	0,00	0,00	1,50	0,20	0,00	0,00	3,10	0,40	0,20	0,00	4,50	0,70	0,10	0,00	5,90	1,10	0,20	0,00
3 ms⁻¹	-4,50	1,00	0,10	0,00	0,00	0,80	0,10	0,00	3,00	0,60	0,10	0,00	6,80	0,90	0,20	0,00	10,10	1,50	0,10	0,00	12,50	2,20	0,10	0,10
4 ms⁻¹	-7,70	1,80	0,10	0,00	0,20	1,30	0,10	0,00	4,90	1,10	0,10	0,00	10,90	1,50	0,10	0,00	16,10	2,40	0,20	0,00	20,00	3,30	0,10	0,10
5 ms⁻¹	-12,40	3,50	0,10	0,10	0,60	2,20	0,20	0,00	8,00	1,90	0,10	0,10	17,10	2,50	0,30	0,10	25,20	3,80	0,20	0,10	32,00	5,10	0,10	0,10

Table #4: Processed data for 'SLOW' model

AIRSPEED	-4°				0°				4°				8°				12°				16°			
α →	L/g	D/g	LD⁻¹	R/g	L/g	D/g	LD⁻¹	R/g	L/g	D/g	LD⁻¹	R/g	L/g	D/g	LD⁻¹	R/g	L/g	D/g	LD⁻¹	R/g	L/g	D/g	LD⁻¹	R/g
1 ms⁻¹	-0,50	0,26	-1,92	0,56	0,00	0,20	0,00	0,20	0,60	0,05	12,00	0,60	1,10	0,10	11,00	1,10	1,60	0,34	4,71	1,64	2,00	0,58	3,45	2,08
2 ms⁻¹	-1,90	0,44	-4,32	1,95	0,00	0,40	0,00	0,40	1,50	0,33	4,55	1,54	3,10	0,67	4,63	3,17	4,50	1,10	4,09	4,63	5,90	1,62	3,64	6,12
3 ms⁻¹	-4,50	0,61	-7,38	4,54	0,00	0,80	0,00	0,80	3,00	0,86	3,49	3,12	6,80	1,50	4,53	6,96	10,10	2,39	4,23	10,38	12,50	3,30	3,79	12,93
4 ms⁻¹	-7,70	1,13	-6,81	7,78	0,20	1,32	0,15	1,34	4,90	1,53	3,20	5,13	10,90	2,46	4,43	11,17	16,10	3,82	4,21	16,55	20,00	5,06	3,95	20,63
5 ms⁻¹	-12,40	2,43	-5,10	12,64	0,60	2,26	0,27	2,34	8,00	2,61	3,07	8,41	17,10	4,01	4,26	17,56	25,20	6,02	4,19	25,91	32,00	7,92	4,04	32,97

Chart #3: R versus airspeed for 'SLOW' model
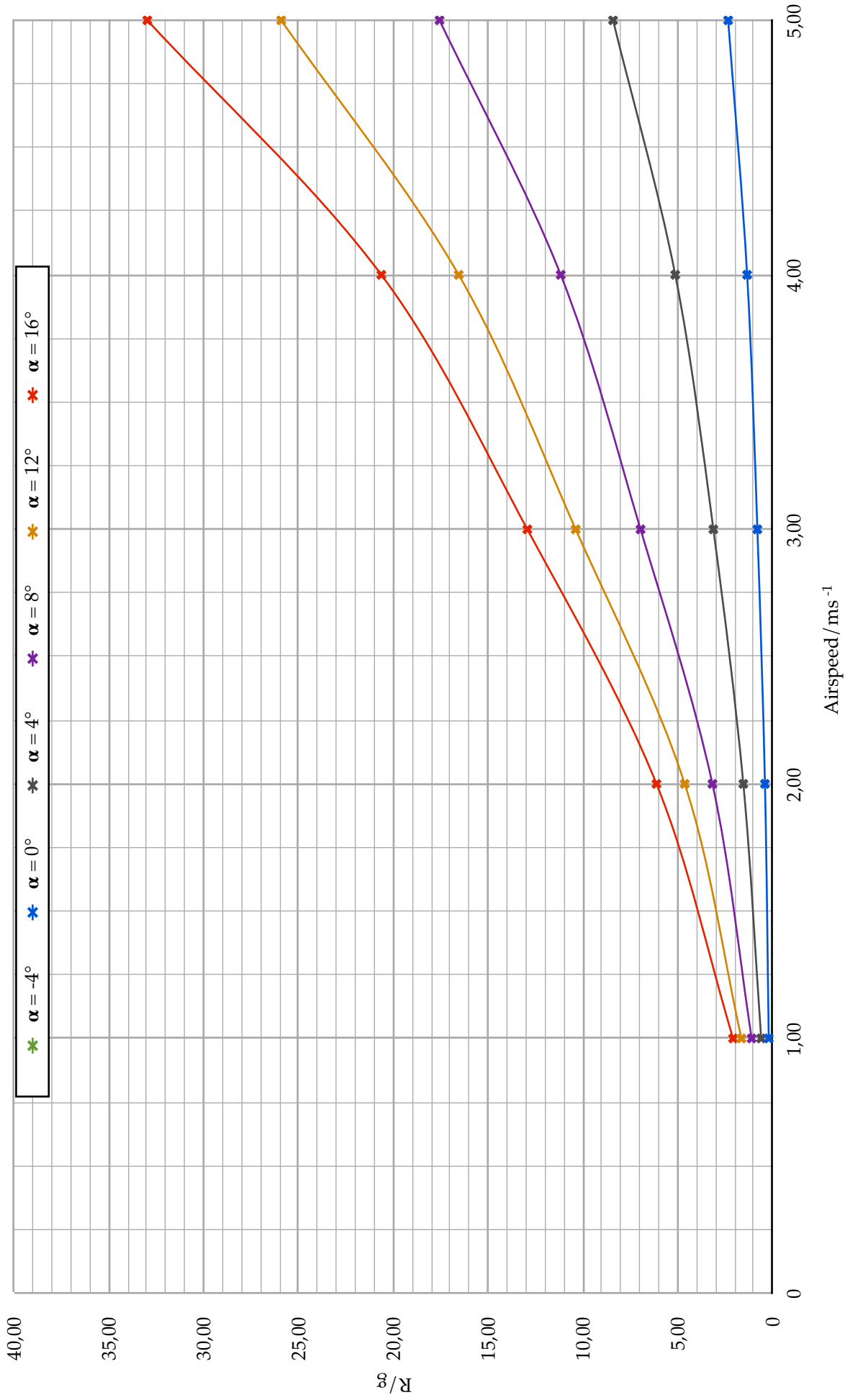
Chart #4: L/D ratio versus airspeed for 'SLOW' model
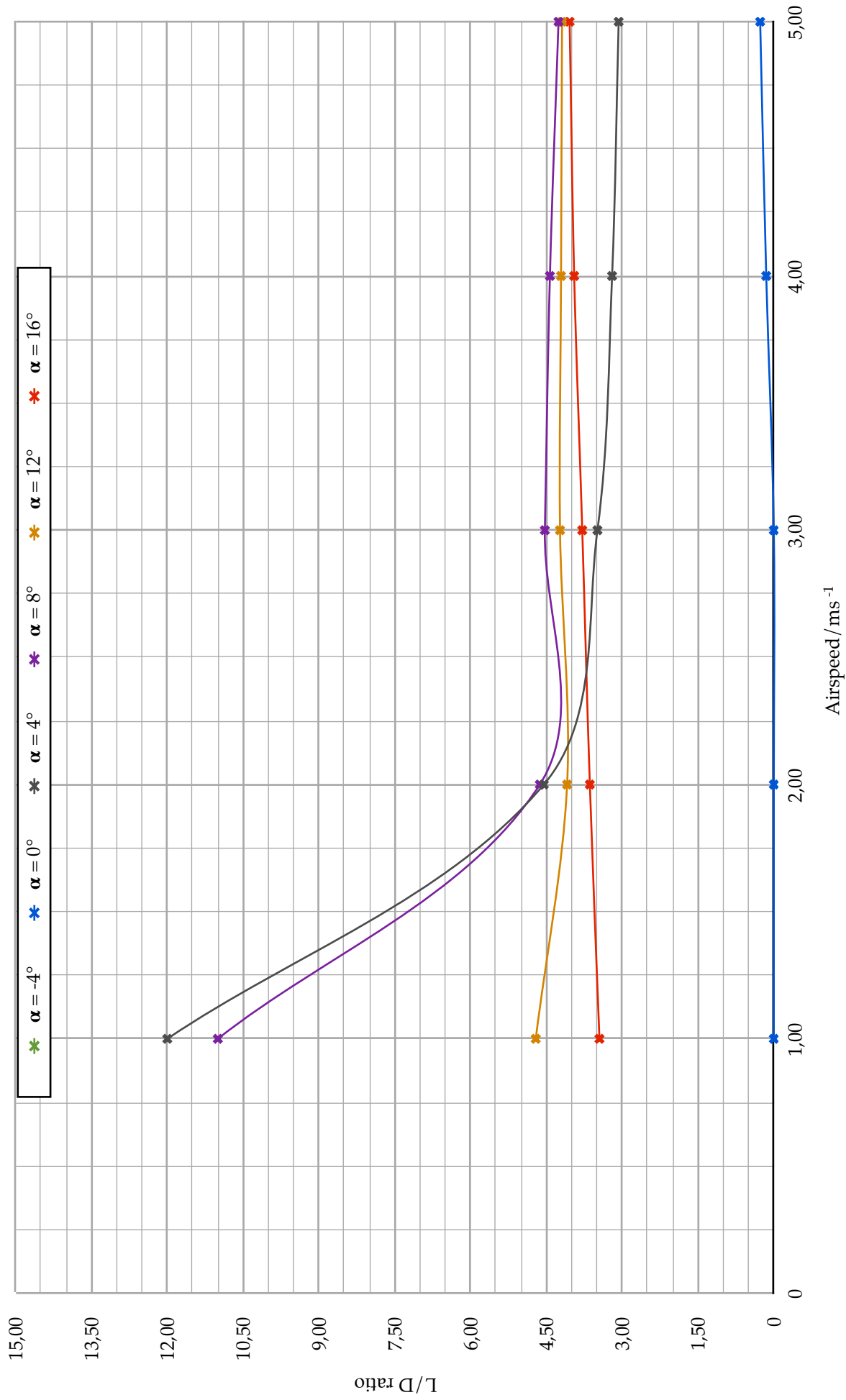
'DART' model:

Table #5: Raw data for 'DART' model

α → AIRSPEED	-4° L/g	D/g	±L	±D	0° L/g	D/g	±L	±D	4° L/g	D/g	±L	±D	8° L/g	D/g	±L	±D	12° L/g	D/g	±L	±D	16° L/g	D/g	±L	±D
1 ms⁻¹	0,20	0,20	0,00	0,00	0,90	0,30	0,10	0,00	1,10	0,20	0,10	0,00	1,50	0,20	0,00	0,00	1,90	0,20	0,10	0,00	2,40	0,40	0,10	0,00
2 ms⁻¹	0,20	0,40	0,10	0,00	1,60	0,40	0,10	0,00	2,40	0,40	0,10	0,00	3,40	0,50	0,20	0,00	4,80	0,80	0,10	0,00	6,30	1,00	0,30	0,00
3 ms⁻¹	0,00	0,60	0,00	0,00	2,50	0,70	0,10	0,00	4,50	0,70	0,30	0,00	7,10	0,80	0,30	0,00	9,90	1,60	0,20	0,00	13,30	2,20	0,30	0,00
4 ms⁻¹	-0,20	1,10	0,20	0,00	3,80	1,20	0,20	0,00	7,00	1,10	0,30	0,00	11,00	1,30	0,30	0,00	16,10	2,70	0,30	0,00	20,90	3,70	0,40	0,10
5 ms⁻¹	-0,50	1,90	0,40	0,00	5,50	2,00	0,40	0,10	10,70	1,90	0,50	0,10	17,80	2,40	0,40	0,10	25,60	4,30	0,50	0,10	33,20	5,90	0,50	0,10

Table #6: Processed data for 'DART' model

| α → AIRSPEED	-4° L/g	D/g	LD⁻¹	R/g	0° L/g	D/g	LD⁻¹	R/g	4° L/g	D/g	LD⁻¹	R/g	8° L/g	D/g	LD⁻¹	R/g	12° L/g	D/g	LD⁻¹	R/g	16° L/g	D/g	LD⁻¹	R/g
1 ms⁻¹	0,20	0,22	0,91	0,30	0,90	0,38	2,37	0,98	1,10	0,30	3,67	1,14	1,50	0,33	4,55	1,54	1,90	0,37	5,14	1,94	2,40	0,61	3,93	2,48
2 ms⁻¹	0,20	0,42	0,48	0,47	1,60	0,54	2,96	1,69	2,40	0,61	3,93	2,48	3,40	0,80	4,25	3,49	4,80	1,22	3,93	4,95	6,30	1,55	4,06	6,49
3 ms⁻¹	0,00	0,60	0,00	0,60	2,50	0,92	2,72	2,66	4,50	1,10	4,09	4,63	7,10	1,42	5,00	7,24	9,90	2,47	4,01	10,20	13,30	3,37	3,95	13,72
4 ms⁻¹	-0,20	1,90	-0,11	1,91	3,80	1,54	2,47	4,10	7,00	1,72	4,07	7,21	11,00	2,27	4,85	11,23	16,10	4,12	3,91	16,62	20,90	5,54	3,77	21,62
5 ms⁻¹	-0,50	1,86	-0,27	1,93	5,50	2,49	2,21	6,04	10,70	2,84	3,77	11,07	17,80	3,97	4,48	18,24	25,60	6,56	3,90	26,43	33,20	8,83	3,76	34,35

Chart #5: R versus airspeed for 'DART' model
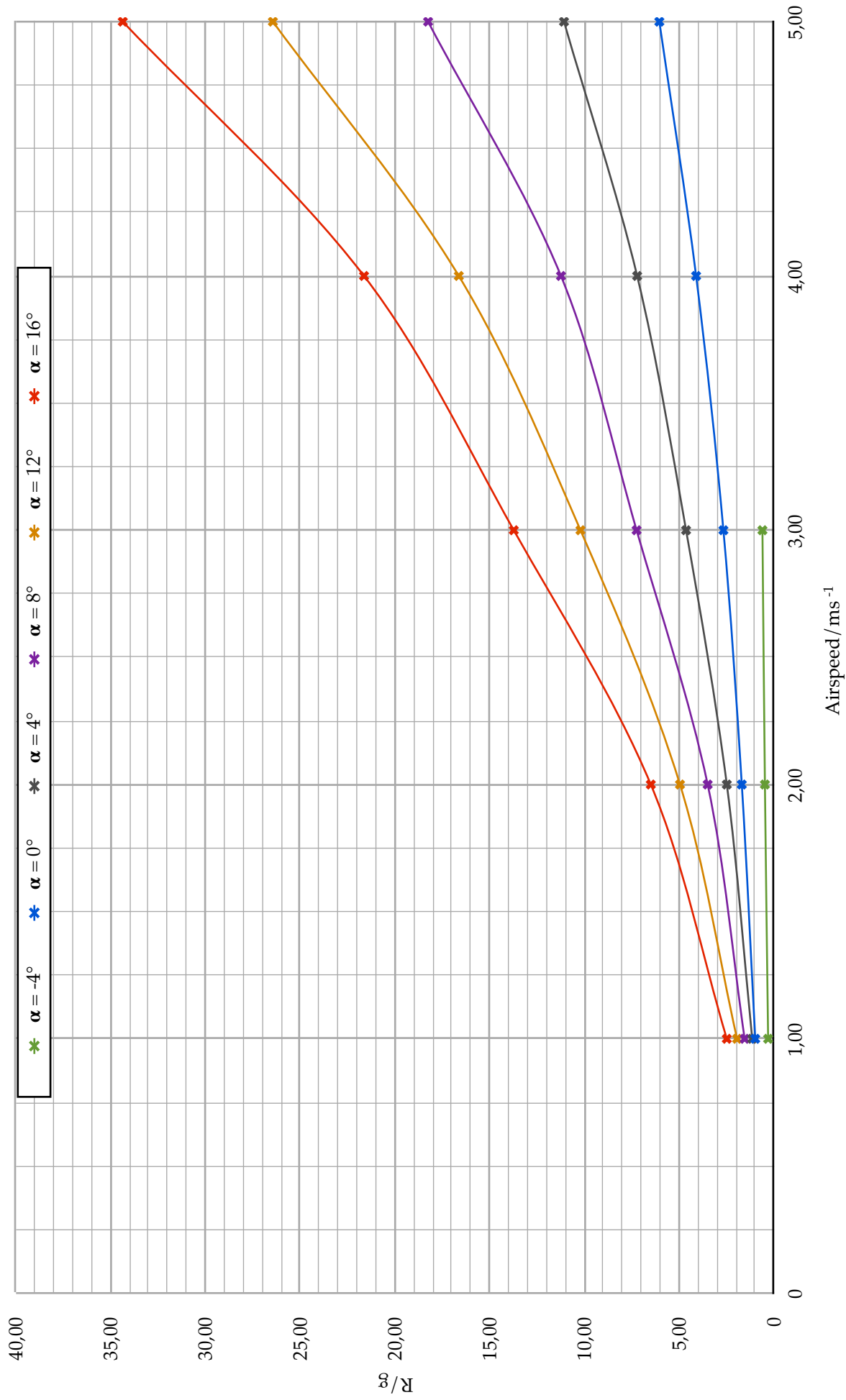
Chart #6: L/D ratio versus airspeed for 'DART' model

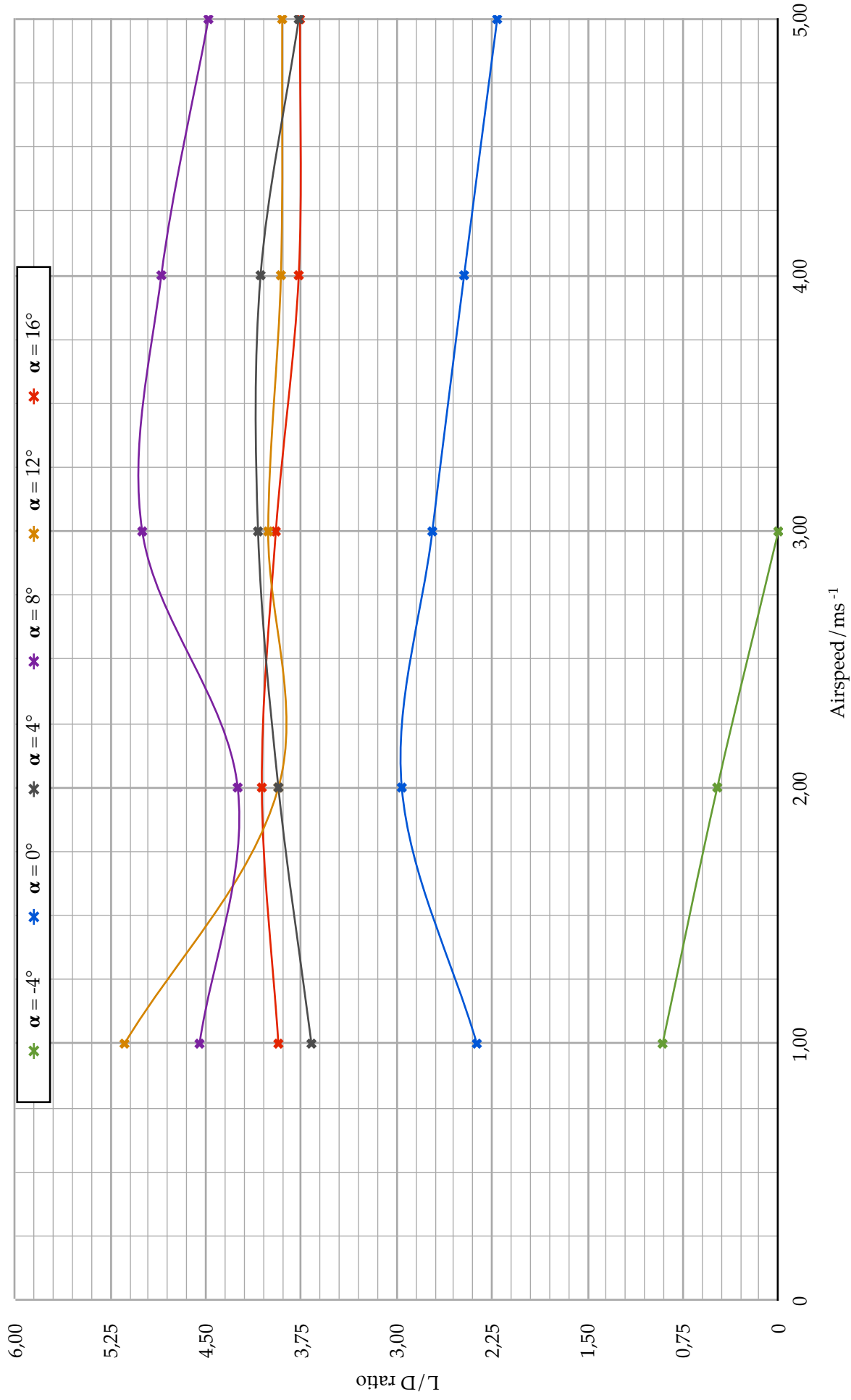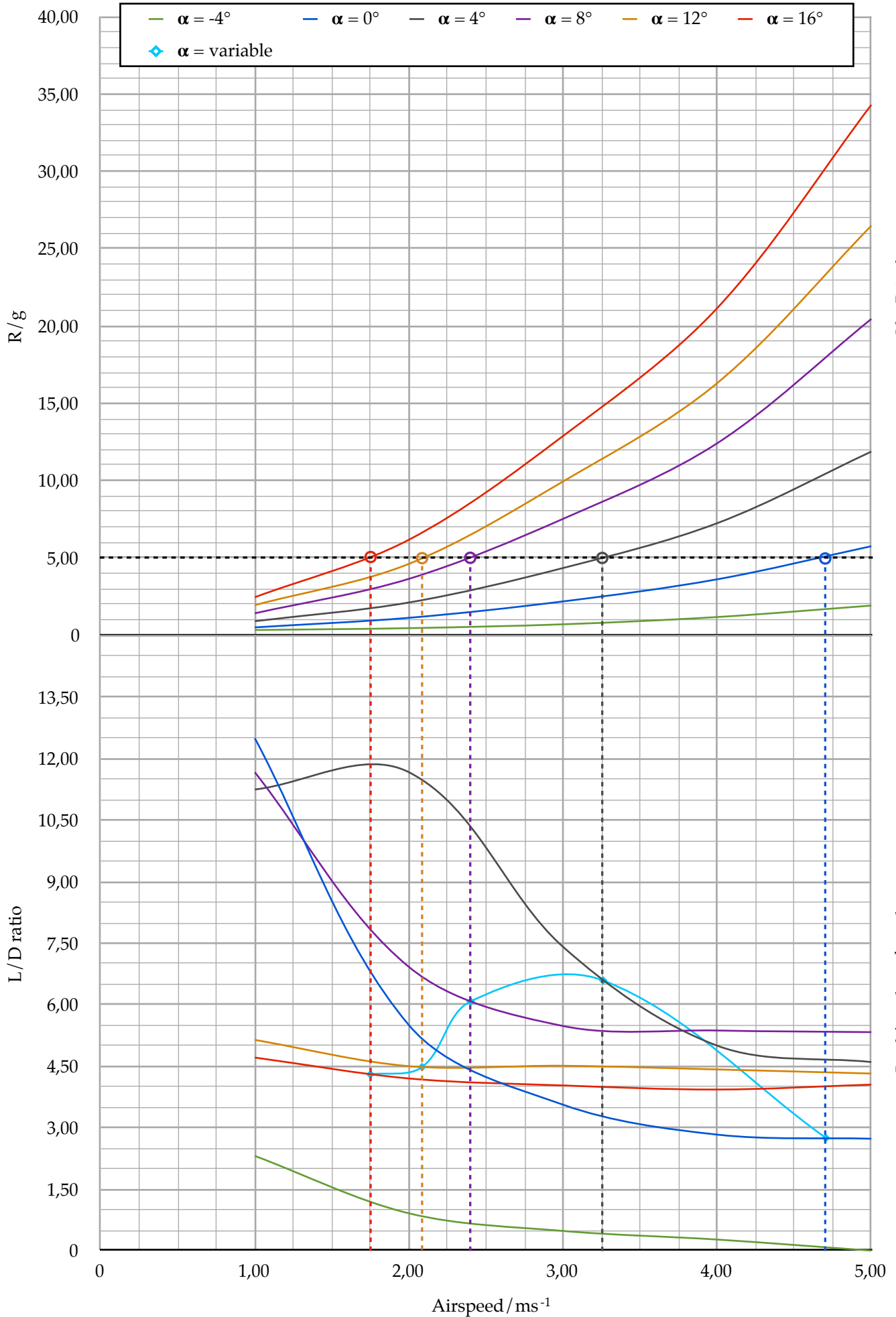*Chart #7: Building L/D curve for the case of uncontrolled engle of attack for 'CLASSIC' model; mass = 5g*

Legend:
- α = -4°
- α = 0°
- α = 4°
- α = 8°
- α = 12°
- α = 16°
- α = variable

Y-axis (top): R/g — 40,00 / 35,00 / 30,00 / 25,00 / 20,00 / 15,00 / 10,00 / 5,00 / 0

Y-axis (bottom): L/D ratio — 13,50 / 12,00 / 10,50 / 9,00 / 7,50 / 6,00 / 4,50 / 3,00 / 1,50 / 0

X-axis: Airspeed / ms⁻¹ — 0 / 1,00 / 2,00 / 3,00 / 4,00 / 5,00

Appendix

Ilya Gulko (001414 -0020)

Ib Diploma

Bedford school

Chart #8: Building L/D curve for the case of uncontrolled engle of attack for 'SLOW' model; mass = 5g
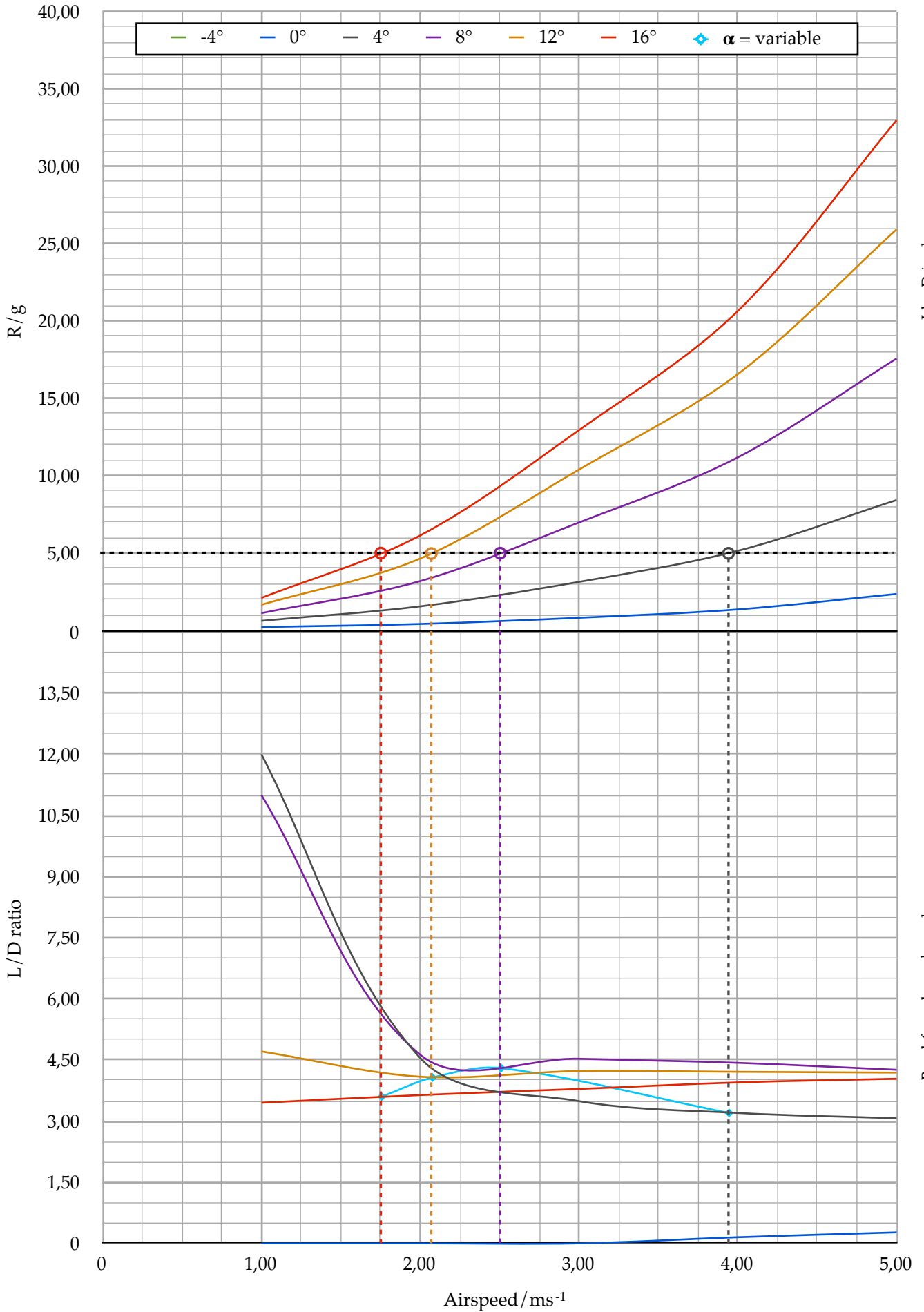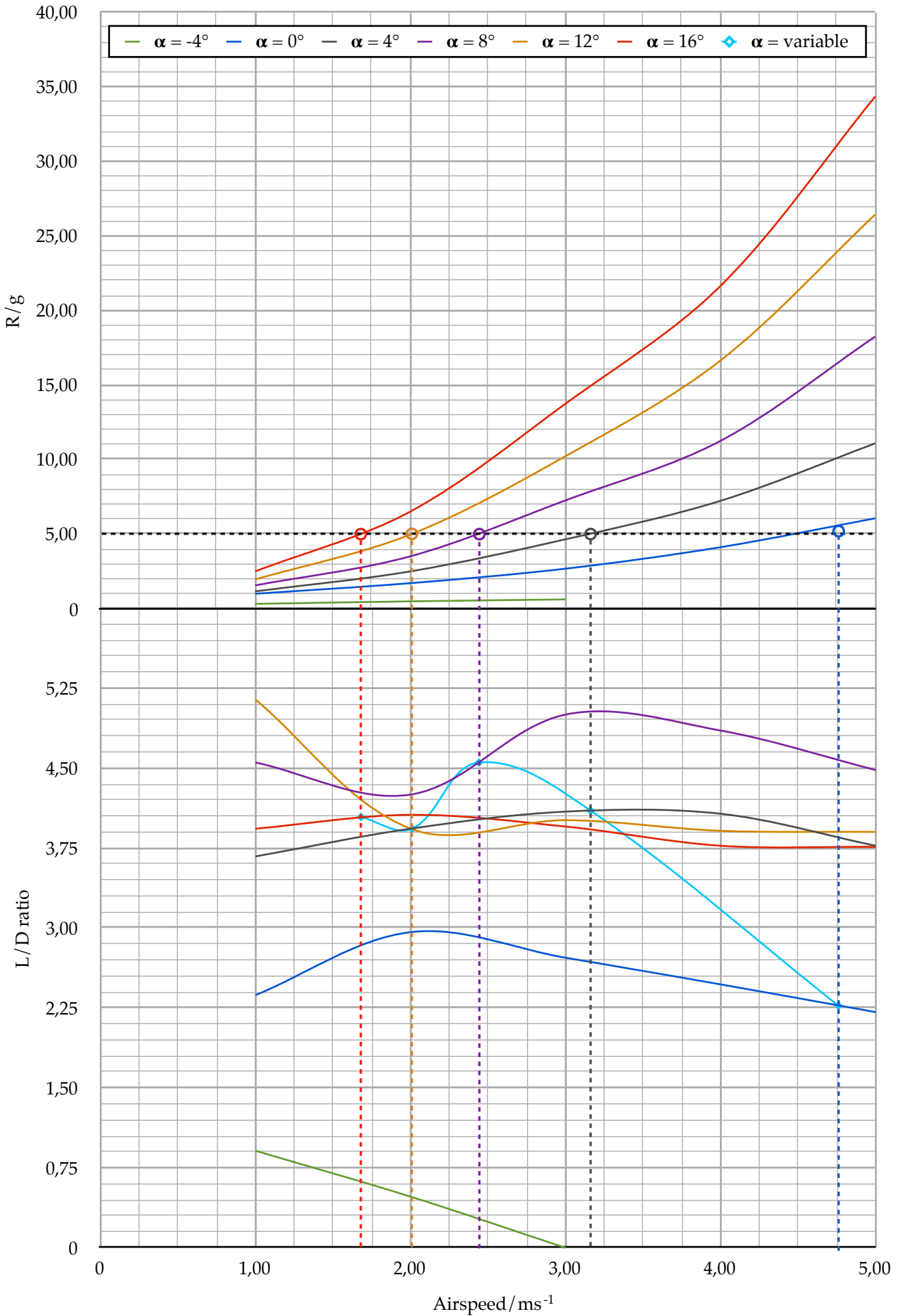
Chart #9: Building L/D curve for the case of uncontrolled engle of attack for 'DART' model; mass = 5g